Transition from Spherical to Deformed Shapes of Nuclei in the Monte Carlo Shell Model

Noritaka Shimizu,[1,2] Takaharu Otsuka,[1,2] Takahiro Mizusaki,[3] and Michio Honma[4]

[1]*Department of Physics, University of Tokyo, Hongo, Tokyo 113-0033, Japan*
[2]*RIKEN, Hirosawa, Wako-shi, Saitama 351-0198, Japan*
[3]*Department of Law, Senshu University, Higashimita, Tama, Kawasaki, Kanagawa, 214-8580, Japan*
[4]*Center for Mathematical Sciences, University of Aizu, Tsuruga, Ikki-machi, Aizu-Wakamatsu, Fukushima 965-8580, Japan*

(Received 27 July 2000)

The transition from spherical to deformed shapes is studied in terms of large-scale shell-model calculations for Ba isotopes as a function of valence nucleon number with fixed single-particle space and Hamiltonian. A new version of the Monte Carlo shell model is introduced so as to incorporate pairing correlations efficiently, by utilizing condensed pair bases. The energy levels and electromagnetic matrix elements are described in agreement with experiments throughout the transitional region. The orbital $M1$ sum rule is calculated as a measure of the deformation evolution, and the Q-phonon picture is shown to be reasonable from spherical to deformed nuclei.

DOI: 10.1103/PhysRevLett.86.1171 PACS numbers: 21.60.Cs, 21.60.Ka, 24.10.Cn, 27.60.+j

The atomic nucleus exhibits a unique and characteristic feature that, although the nucleus is a highly quantal many-body system, it has a rather distinct shape. This shape can be a sphere, an ellipsoid, or an object in between, depending on the numbers of protons and neutrons. In nuclei at or near closed shells, the ground state is spherical, while the "phase" transition [1] from the spherical to the deformed shapes occurs gradually as the nucleus moves away from closed shells on the nuclear chart. This phase transition affects properties of certain low-lying states, and those states are called "quadrupole collective states," because the deformation is primarily of quadrupole nature and the shape is directly linked to the collective motion of nucleons. Because of this collectivity, one has to study the structure of heavy nuclei with many valence nucleons, in order to investigate the phase transition precisely. In fact, such studies have been carried out over decades both phenomenologically and microscopically, but a microscopic calculation covering the transitional region in a chain of heavy nuclei (e.g., isotopic chain) has so far been missing, because dynamical many-body correlations are quite important in the transitional region, but the evaluation of such correlations inevitably requires a theoretical framework beyond the mean field approaches. We further note that the RPA (or TDA) calculation can be used for a certain lowest vibrational state but not for higher states. On the other side, the nuclear shell model is a natural choice for such studies, because all dynamical effects within the given Hilbert space are treated equally well and also because the full spectrum can be calculated in principle. For heavy nuclei exhibiting prominent shape phase transition, however, the Hamiltonian matrix becomes too large to be diagonalized.

In this study, we present the first result of the Monte Carlo shell model (MCSM) [2–8] applied to quadrupole collective states of heavy nuclei, focusing on the shape phase transition. The Monte Carlo shell model stands for applications of the quantum Monte Carlo diagonalization method to the nuclear shell model. It will be demonstrated that, by changing the number of valence particles, the shape phase transition indeed occurs quite prominently in heavy nuclei, while the Hamiltonian and the single-particle orbits are being kept unchanged. Thus, this work provides us with the first evidence, by means of microscopic calculations beyond mean field approaches, that the shape phase transition can occur due to the change of valence particle number with a realistic Hamiltonian and shell structure.

The isotopic chain of Ba isotopes with $N \geq 82$ is chosen as an example, because the shape phase transition is seen clearly in experiments between ^{138}Ba, a semimagic spherical nucleus, and ^{148}Ba, a rotational deformed nucleus [9–13]. Only even-N isotopes are studied. The full major shells are taken: $50 \leq Z \leq 82$ for protons and $82 \leq N \leq 126$ for neutrons. For ^{146}Ba, the deformation parameter deduced experimentally is $\beta_2 \sim 0.22$ [14]. For heavier Ba isotopes, β_2 is probably somewhat larger, but for such values the closed shell of $Z = 50$ and $N = 82$ appears to be still stable in the Nilsson diagram. The energy spectrum becomes, towards ^{150}Ba, very close to a rotational one with axial symmetry. Thus, Ba isotopes with $N \geq 82$ turn out to be quite appropriate for the present study. One may have to be cautious of the validity of the closed shell for nuclei with $Z > 56$ and $N \sim 92$ because of stronger deformation.

The MCSM is devised so that one can extract important many-body bases out of the entire Hilbert space by using a stochastic method and can then diagonalize the Hamiltonian in the subspace spanned by these bases [2–5]. Thus, in the MCSM, most important bases for describing an assigned eigenstate are generated. The MCSM can hence be referred to as an *importance truncation* scheme [6]. Many-body bases are given in the form of Slater determinants in the existing MCSM calculations [2–8]. In the present study, we investigate the structure of heavy nuclei where the pairing correlation plays a crucial role: the

many-body basis is given in the form of a pair-condensed state,

$$|\phi\rangle = (\Lambda)^{\dagger N}|-\rangle, \tag{1}$$

where N is half the particle number, $|-\rangle$ means the closed shell (i.e., inert core), $\Lambda^\dagger$ is the creation operator of a pair of nucleons,

$$\Lambda^\dagger = \sum_{ij} \lambda_{ij} c_i^\dagger c_j^\dagger, \tag{2}$$

with $c_i^\dagger$ being the creation operator of a nucleon and λ_{ij} denoting amplitudes. By having different sets of λ's, one can have independent basis states, which span a subspace for diagonalizing the Hamiltonian. If one generates sufficient bases, the result becomes a good approximation. In this work, pairs of neutrons and pairs of protons are considered, whereas proton-neutron pairs are not.

If one chooses the amplitude λ's to be consistent with the u and v factors of the BCS (HFB, i.e., Hartree-Fock Bogoliubov) formalism [1], the state $|\phi\rangle$ becomes identical to the number projected BCS (HFB) ground state. Thus, the new form of many-body basis can include pairing correlations more efficiently.

The basis states are generated in the same way as in the standard MCSM [2–5]:

$$|\phi(\sigma)\rangle = U(\sigma)\,|\phi^{(0)}\rangle, \qquad U(\sigma) \equiv \prod_{n=1}^{N_t} e^{-\Delta\beta h(\sigma_n)}, \tag{3}$$

where σ denotes a set of random numbers (i.e., auxiliary fields), $|\phi^{(0)}\rangle$ indicates an initial state, and $h(\sigma)$ means one-body Hamiltonian [2]. Here, $\Delta\beta$ and N_t are parameters regarding the imaginary time evolution and can be tuned for more efficient computation.

As the initial state, the HFB ground state is taken in the present work. The operator U in Eq. (3) transforms $c_i^\dagger c_j^\dagger$ in Eq. (2) to $Uc_i^\dagger U^{-1} Uc_j^\dagger U^{-1}$. Note that U is nothing but an exponential function of a one-body operator and hence transforms a single-particle state to a linear combination of single-particle states.

There are several options for the basis generation as discussed in [5]. In this paper, we adopt *J-compressed bases* for which the angular-momentum projection is fully implemented, giving the best accuracy [5]. We shall refer to the basis $|\phi\rangle$ in Eq. (1) as the pair basis, in order to distinguish from the basis given in the form of Slater determinant. A similar type of bases is used in the VAMPIR calculation [15].

We introduce the axial symmetry. This symmetry means that the basis does not change with respect to the rotation about an axis. The z axis is chosen as this symmetry axis. In many deformed nuclei, this symmetry is found in low-lying states, while the ground state and its vibrational excitations of spherical nuclei can be described in terms of axially symmetric bases because all orientations are included through the angular momentum projection. The validity of this assumption is discussed later in some detail. The single-particle states i and j in Eq. (2) are defined to have a good z component of the angular momentum, denoted M_i and M_j, respectively. Because of the axial symmetry, the z component of the angular momentum of the Λ pair in Eq. (2) is zero, i.e.,

$$\lambda_{ij} = 0 \quad \text{for } M_i + M_j \neq 0\,. \tag{4}$$

We next sketch the method for calculating matrix elements. The matrix elements of the unit, one-body, two-body operators should be calculated between pair bases. This can be worked out recursively by contracting nucleon pairs as described in [16]. We introduce a pair $\Omega^\dagger = \omega_{ij} c_i^\dagger c_j^\dagger$. The matrix of λ_{ij} and ω_{ij} are denoted by λ and ω. For instance, the overlap, $I^{(N)}$, between the condensed states of the pairs Λ and Ω is given as

$$\begin{aligned} I^{(N)} &\equiv \langle -|\Omega^N (\Lambda^\dagger)^N|-\rangle \\ &= -\frac{N}{2} \sum_{l=0}^{N-1} \left[\frac{N!}{(N-l)!}\right]^2 I^{(N-l)}. \end{aligned} \tag{5}$$

Those recursive formulas enable us to calculate values of various matrix elements conserving the particle number. We note that, for number-violating HFB wave functions, one has to use a projection method like the one of [17].

Now we discuss the structure of $^{138-150}$Ba nuclei. Single particle orbits, $2s_{1/2}$, $1d_{5/2}$, $1d_{3/2}$, $0g_{7/2}$, and $0h_{11/2}$ are taken for protons. Those for neutrons are $2p_{3/2}$, $2p_{1/2}$, $1f_{7/2}$, $1f_{5/2}$, $0h_{9/2}$, and $0i_{13/2}$. The single particle energies are adopted from the experimental energy levels of ^{133}Sn [18] for neutrons and from those of ^{133}Sb [19] for protons. The two-body effective interaction between identical nucleons is assumed to be comprised of the monopole pairing, quadrupole pairing, and quadrupole-quadrupole interactions, the strengths of which are denoted as $g^{(0)}$, $g^{(2)}$, and $f^{(2)}$, respectively. These parameters are defined in the usual way as can be seen also in [16]. The values of these strengths for protons (neutrons) are fitted so as to reproduce the energy levels of semimagic nuclei such as $N = 82$ isotones (^{134}Sn). Note that levels of Sn isotopes heavier than ^{134}Sn have not been observed. The adopted values for neutrons (protons) are $g^{(0)} = 0.13$ (0.21) MeV, $g^{(2)} = 0.14$ (0.22) MeV, and $f^{(2)} = -0.0002$ (-0.0002) MeV/fm^4, respectively. Since $f^{(2)}$ is small and has only minor effects, for simplicity, its value for neutrons is taken to be equal to that for protons. The resultant levels of ^{134}Sn are 0.76, 1.26, and 1.26 MeV for the 2_1^+, 4_1^+, and 6_1^+ states, respectively. Their experimental values are quite close: 0.73, 1.07, and 1.25 MeV, respectively [20]. The levels of $N = 82$ isotones are also well reproduced, as presented for ^{138}Ba [9] below. The proton-neutron interaction is assumed to consist of the quadrupole-quadrupole interaction. The strength of this interaction is the only parameter needed to be adjusted with $N > 82$ Ba isotopes. Its value was taken as $f^{(2)} = -0.0014$ MeV/fm^4, so as to reproduce the 2_1^+ level of ^{148}Ba. The values of these interaction strengths turn out to be reasonable from the viewpoint of systematics. Note that the proton-neutron quadrupole interaction is much stronger than the neutron-neutron

or proton-proton one, which is actually a well-known property. All these interaction strengths are kept constant throughout the whole calculations below, as expected for the effective interaction.

Figure 1 shows energy levels, $E_x(J)$, for yrast states with the spin parity J^+ up to $J = 10$. $E_x(2)$ is as high as 1.5 MeV at $A = 138$, but it sharply drops down as more valence neutrons are added and becomes less than 10% for $A = 148$. This change is reproduced by the MCSM calculation quite well. We emphasize again that only the number of neutrons is varied, while no parameter in the Hamiltonian is adjusted for the change. The experimental energy levels show a vibrational pattern for $A \sim 140$, characterized by the ratio $R \equiv E_x(4)/E_x(2) \sim 2$. This ratio becomes $R \sim 3$ at $A = 148$ experimentally, which is close to the rotational limit with axial symmetry. The rotation is directly connected to the deformation through the Nambu-Goldstone mechanism: an ellipsoid rotates to restore rotational symmetry broken due to the deformation from a sphere. The present calculation reproduces the variation of the ratio R extremely well, indicating that the shape phase transition originates in the change of the neutron number in this case.

Other energy levels are also nicely reproduced by the calculation. We note that the 8^+ level is raised from $A = 144$ to 146 both in experiment and in calculation. This is actually due to additional binding of lower states.

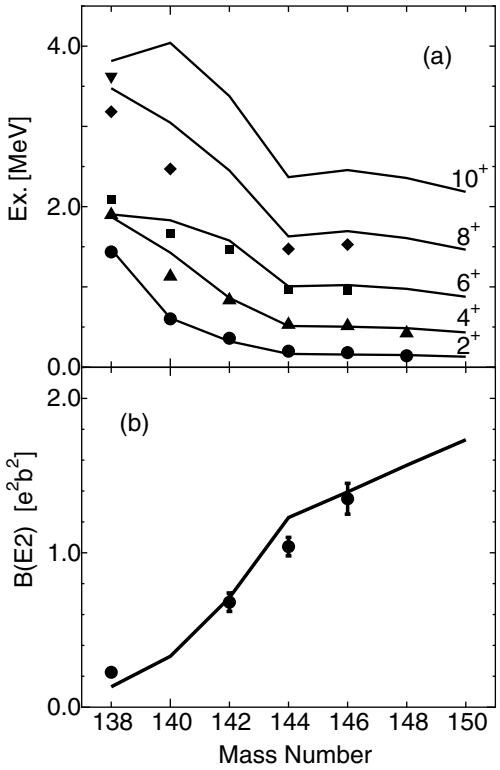

FIG. 1. (a) Energy levels of Ba isotopes. The lines are calculations, while the symbols represent experiments [9–13]. (b) $B(E2; 0_1^+ \rightarrow 2_1^+)$ values of Ba isotopes. Symbols are experimental [14], while the line is calculation.

At this stage, we examine the assumption of the axial symmetry. Experimental data for even-N Ba isotopes with $N > 82$ are consistent with this assumption. For instance, the 2_2^+ level is well above the 4_1^+ level for all those isotopes. This assumption is examined within the theoretical calculation as well. We take the 6^+ state of ^{140}Ba as an example. First, 20 bases are generated with the axial symmetry. We then generate another 20 bases with various triaxial deformation. We combine these triaxial bases with the bases with the axial symmetry and span a larger Hilbert subspace. The energy eigenvalue is then lowered only by about 10 keV, which is rather small compared to the 6^+ excitation energy, 1.83 MeV. Note that there are certain nuclei where the axial symmetry is not valid and such nuclei are described by bases without this symmetry in the MCSM [21].

We now turn to $E2$ transitions. Figure 1 shows also values of $B(E2; 0_1^+ \rightarrow 2_1^+)$. Since this quantity is nothing but the square of the transition matrix element of the $E2$ moment operator, it becomes larger as the quadrupole deformation becomes stronger. In fact, this value grows rapidly as the neutron number increases, in agreement with experimental values. This increase of $B(E2; 0_1^+ \rightarrow 2_1^+)$ by an order of magnitude between two ends is another indication of the shape phase transition. The effective charges are taken to be $1.6e$ for protons and $0.6e$ for neutrons. The spectroscopic $E2$ moments are calculated, exhibiting a similar trend.

The $M1$ strength to the scissors mode can be a good measure of the deformation of the ground state [22,23]. This $M1$ strength is mainly due to the orbital contribution in the $M1$ transition. We calculate the $M1$ sum rule for the ground state with the orbital g factors having the free nucleon values (i.e., 1 for protons and 0 for neutrons). The spin contributions are omitted for simplicity. In Fig. 2, the $B(M1)$ sum rule thus obtained is plotted vs the corresponding $B(E2; 0_1^+ \rightarrow 2_1^+)$ value. One finds a nearly perfect linearity between the two quantities. This seems to be the first microscopic calculation of this relation throughout

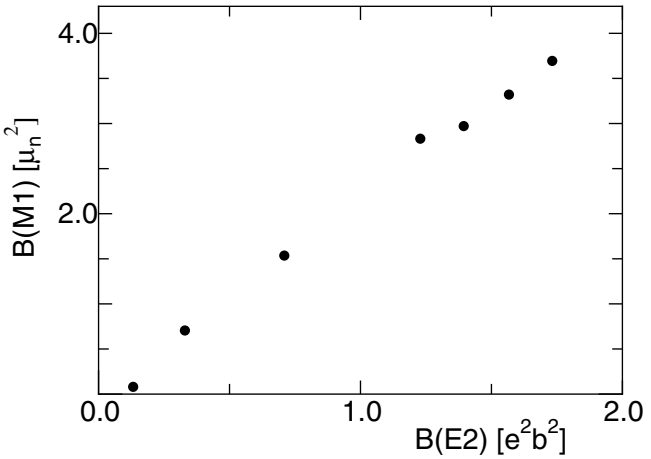

FIG. 2. Orbital $B(M1)$ sum rule from the ground state plotted vs the corresponding $B(E2; 0_1^+ \rightarrow 2_1^+)$ value in Ba isotopes.

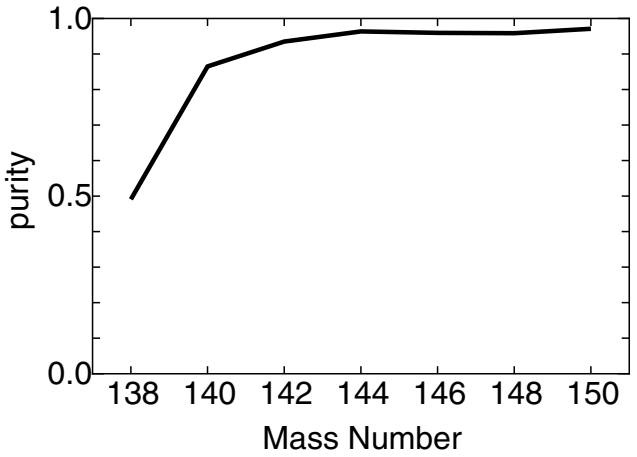

FIG. 3. Q-phonon purity as a function of the mass number for Ba isotopes.

the transitional region. The linear relation between the above $B(M1)$ and $B(E2)$ has been derived based on the intrinsic deformation [22]. It is now shown to be valid in the transitional region where such a static deformation picture may not be applicable.

The structure of the wave function of quadrupole collective states can be analyzed in terms of the Q-phonon picture, which has been introduced originally for the γ-unstable nuclei [24]. In the Q-phonon scheme, the 2_1^+ state is constructed by applying an appropriate quadrupole operator on the ground state. We here define the Q-phonon purity

$$P \equiv \frac{|\langle 2_1^+ || Q || 0_1^+ \rangle|^2}{\sum_i |\langle 2_i^+ || Q || 0_1^+ \rangle|^2}, \tag{6}$$

where Q stands for the isoscalar quadrupole operator. Figure 3 shows the Q-phonon purity for the Ba isotopes. At $A = 138$, P is only about half, but P becomes about 0.9 for $A = 140$ and about 0.95 for $A \geq 140$. This result indicates that the Q-phonon scheme becomes a good approximation for constructing the wave function once both valence protons and valence neutrons are present. This property has been suggested by using observed $B(E2)$ values [25], while it has never been studied by microscopic calculations.

In summary, we have developed a new version of the MCSM calculation with condensed pair bases. This version enables us to carry out the shell-model calculations for heavier nuclei which have collective properties and pairing correlations. We studied the shape phase transition in the Ba isotopes, presenting this phenomenon quite nicely with fixed Hamiltonian and single-particle space. Namely, the variation of the valence particle number is the driving force of the phase transition. The phase transition is clearly seen through energy levels and $E2$ transitions. The scissors orbital $M1$ strength is confirmed microscopically to be a clean physical quantity. The Q-phonon scheme is shown to be a reasonable approximation for a wide range of nuclei. More systematic studies with a more realistic effective interaction will be of particular interest.

This work was supported in part by Grant-in-Aid for Scientific Research (A)(2) (10304019) from the Ministry of Education, Science and Culture. The numerical calculations were carried out in part by the Alphleet computer in RIKEN.

[1] P. Ring and P. Schuck, *The Nuclear Many-Body Problem* (Springer-Verlag, Berlin, 1980), p. 380.
[2] M. Honma, T. Mizusaki, and T. Otsuka, Phys. Rev. Lett. **75**, 1284 (1995).
[3] T. Mizusaki, M. Honma, and T. Otsuka, Phys. Rev. C **53**, 2786 (1996).
[4] M. Honma, T. Mizusaki, and T. Otsuka, Phys. Rev. Lett. **77**, 3315 (1996).
[5] T. Otsuka, M. Honma, and T. Mizusaki, Phys. Rev. Lett. **81**, 1588 (1998).
[6] T. Otsuka, M. Honma, and T. Mizusaki, J. Phys. G **25**, 699 (1999).
[7] T. Mizusaki, T. Otsuka, Y. Utsuno, M. Honma, and T. Sebe, Phys. Rev. C **59**, R1846 (1999).
[8] Y. Utsuno, T. Otsuka, T. Mizusaki, and M. Honma, Phys. Rev. C **60**, 054315 (1999).
[9] M. A. Islam, T. J. Kennett, and W. V. Prestwich, Phys. Rev. C **42**, 207 (1990).
[10] L. J. Alquist, W. C. Schick, Jr., W. L. Talbert, Jr., and S. A. Williams, Phys. Rev. C **13**, 1277 (1976).
[11] S. M. Scott *et al.,* J. Phys. G **6**, 1291 (1980).
[12] W. Urban *et al.,* Nucl. Phys. **A613**, 107 (1997).
[13] J. C. Hill *et al.,* Phys. Rev. C **34**, 2312 (1986).
[14] S. Raman, C. H. Marlarkey, W. T. Milner, C. W. Nestor, Jr., and P. H. Stelson, At. Data Nucl. Data Tables **36**, 1 (1987).
[15] A. Petrovici, K. W. Schmid, and A. Faessler, Nucl. Phys. **A665**, 333 (2000), and references therein.
[16] T. Mizusaki and T. Otsuka, Prog. Theor. Phys. Suppl. **125**, 97 (1996).
[17] K. Neergaard and E. Wuest, Nucl. Phys. **A402**, 311 (1983).
[18] P. Hoff *et al.,* Phys. Rev. Lett. **77**, 1020 (1996).
[19] L. A. Stone *et al.,* Phys. Scr. **T56**, 316 (1995).
[20] C. T. Zhang *et al.,* Z. Phys. A **358**, 9 (1997).
[21] N. Shimizu, T. Otsuka, T. Mizusaki, and M. Honma (to be published).
[22] N. Lo Iudice and A. Richter, Phys. Lett. B **304**, 193 (1993).
[23] N. Pietralla, P. von Brentano, R.-D. Herzberg, U. Kneissl, N. Lo Iudice, H. Maser, H. H. Pitz, and A. Zilges, Phys. Rev. C **58**, 184 (1998).
[24] T. Otsuka and K.-H. Kim, Phys. Rev. C **50**, 1768 (1994).
[25] N. Pietralla, P. von Brentano, R. F. Casten, T. Otsuka, and N. V. Zamfir, Phys. Rev. Lett. **73**, 2962 (1994).